Mining recent brain proteomic databases for ion channel phosphosite nuggets

Oscar Cerda, ¹ Je-Hyun Baek, ¹ and James S. Trimmer ^{1,2}

¹Department of Neurobiology, Physiology, and Behavior and ²Department of Physiology and Membrane Biology, University of California, Davis, Davis, CA 95616

Voltage-gated ion channels underlie electrical activity of neurons and are dynamically regulated by diverse cell signaling pathways that alter their phosphorylation state. Recent global mass spectrometric–based analyses of the mouse brain phosphoproteome have yielded a treasure trove of new data as to the extent and nature of phosphorylation of numerous ion channel principal or α subunits in mammalian brain. Here we compile and review data on 347 phosphorylation sites (261 unique) on 42 different voltage-gated ion channel α subunits that were identified in these recent studies. Researchers in the ion channel field can now begin to explore the role of these novel in vivo phosphorylation sites in the dynamic regulation of the localization, activity, and expression of brain ion channels through multisite phosphorylation of their principal subunits.

INTRODUCTION

The Journal of General Physiology

Voltage-dependent ion channels underlie the electrical signaling that allows for neurotransmission within neurons, and allow for various modes of Ca²⁺ influx critical to coupling this electrical activity to diverse physiological events (Hille, 2001). As such, voltage-gated ion channel activity is highly regulated by diverse neuronal signaling pathways. Neuronal ion channels exist as supramolecular protein complexes composed of poreforming transmembrane principal or α subunits (Yu et al., 2005), auxiliary or regulatory subunits (Hanlon and Wallace, 2002), and a diverse array of interacting proteins (Dai et al., 2009). Diverse posttranslational events acting on each of these components dynamically regulate the expression, localization, and function of neuronal ion channels (Levitan, 2006). While numerous noncovalent mechanisms such as ligand binding, sensing of transmembrane voltage, and interaction with other proteins are known to play prominent roles in regulating neuronal ion channels, direct covalent modification of the component subunits of these multiprotein ion channel complexes by phosphorylation has long been recognized as a widely used and potent mechanism for neurons to achieve dynamic and reversible changes in ion channel function, and to impact their contribution to neuronal signaling (Levitan, 1985).

Phosphorylation constitutes a common covalent post-translational modification in eukaryotes (Cohen, 2001), with (as of early 2009) up to 25,000 described phosphorylation sites (or phosphosites) on 7,000 human

proteins, out of an estimated 500,000 potential phosphosites that exist in a cellular proteome (Lemeer and Heck, 2009). In neurons, reversible activity-dependent phosphorylation represents a major mechanism of dynamic regulation of synaptic development (Saneyoshi et al., 2010), as well as synaptic potentiation, depression, and homeostatic plasticity (Turrigiano, 2008), through phosphorylation of a large number of synaptic proteins including ligand-gated ion channels (Collins and Grant, 2007). Neurons also exhibit cellular plasticity at the level of intrinsic excitability, achieved through phosphorylation of components of ion channel subunits, for example of voltage-gated sodium or Nav (Cantrell and Catterall, 2001) and potassium or Kv (Schulz et al., 2008) channels, which localize in distinct neuronal compartments (Vacher et al., 2008). As opposed to the classical approaches of in vivo or in vitro radiolabeling with ³²P, peptide mapping and/or sequencing, and site-directed mutagenesis (e.g., Costa et al., 1982; Costa and Catterall, 1984), mass spectrometry (MS)-based phosphoproteomic techniques have recently emerged as the primary tool for the identification of phosphorylation on ion channel subunits (Cerda and Trimmer, 2010). While many of these studies continue to rely on effective purification of the target ion channel before analysis, a set of recent studies from the proteomics field, aimed at defining the global phosphoproteome of mouse brain samples with high complexity, and without a focus on ion channels per se, have yielded a dataset that is extremely valuable to the ion

O. Cerda and J.-H. Baek contributed equally to this work. Correspondence to James S. Trimmer: jtrimmer@ucdavis.edu

Abbreviations used in this paper: CID, collision-induced dissociation; IMAC, immobilized metal affinity chromatography; MS, mass spectrometry; SAX, strong anion exchange; SCX, strong cation exchange.

^{© 2010} Cerda et al. This article is distributed under the terms of an Attribution–Noncommercial–Share Alike–No Mirror Sites license for the first six months after the publication date (see http://www.rupress.org/terms). After six months it is available under a Creative Commons License (Attribution–Noncommercial–Share Alike 3.0 Unported license, as described at http://creativecommons.org/licenses/by-nc-sa/3.0/).

channel community. Here we provide an overview of these studies, as well as the subset of these databases that pertain to voltage-gated ion channel α subunits. These studies provide important insights to the ion channel community on the extent and nature of phosphorylation of mammalian brain ion channels, and a wealth of phosphosites that can be tested for their specific role in regulating these ion channels through dynamic and reversible phosphorylation of their principal pore-forming and voltage-sensing α subunits.

Recent innovations in proteomics and bioinformatics have expanded our knowledge to include nearly 10,000 mammalian brain proteins (Wang et al., 2006). Data from such high-throughput proteomic approaches represents information on ion channel expression patterns that could be of great use to the ion channel community, but may not be as readily accessible to the average "channelologist." However, the number of publications describing such "global" analyses is large and ever increasing, and sifting through huge databases to gain information on the spatial and temporal expression patterns of Your Favorite Channel can be tedious and time consuming, although the resultant information can reveal important insights. More recently, analogous high-throughput studies have provided an even rarer gem, the determination of brain peptides chemically modified with phosphate, and the site of phosphorylation within these peptides (Lemeer and Heck, 2009). Such in vivo studies have yielded an enormous dataset of phosphosites, including those on mammalian brain ion channels. (Hereafter, we will refer to such sites as "in vivo phosphosites.") What in the past would take a tremendous amount of effort in purifying the ion channel proteins from brain preparations, and then identifying the phosphosites (using techniques that often used multiple millicuries of ³²P) is now available to the average channelologist at the click of the mouse. That said, one first needs to be aware of the existence of these studies, then search through the accompanying datasets for the presence of Your Favorite Channel, and then perform analyses to determine the site of phosphorylation within specific channel isoforms. This can present a challenge for those more accustomed to a patch clamp rig than a large and complex proteomics dataset. In this brief review, we attempt to first bring these recent studies to the attention of members of the ion channel community, to highlight the wealth of the data being generated by these approaches, and second to detail the subset of the data related to voltage-gated ion channels. The goal is to ensure that the existing data, and others that will emerge from future studies, can be effectively used to gain mechanistic insights into how neuronal ion channels are regulated by reversible phosphorylation at these in vivo phosphosites. Note that this synopsis is assuredly not comprehensive, as there are likely other high-throughput studies that have yielded data leading

to identification of ion channel phosphosites that we have not included in our analyses, which focuses only on data from four recent global analyses from mouse brain (Munton et al., 2007; Trinidad et al., 2008; Tweedie-Cullen et al., 2009; Wisniewski et al., 2010). Moreover, we should mention that the recent establishment of open source curated databases of posttranslational modifications, such as PhosphositePlus (http://www.phosphosite .org), Phosida (http://141.61.102.18/phosida/index .aspx, which currently contains 23,387 proteins and 69,790 identified phosphorylation sites across eukaryotes; Gnad et al., 2007), Phospho.ELM (http://phospho.elm.eu.org; current version 9.0 contains 8,718 substrate proteins from different species covering 42,573 phosphorylation sites; Diella et al., 2004; Diella et al., 2008), and Human Protein Reference Database (http://www.hprd .org, containing 30,047 proteins and 93,710 posttranslational modifications; Amanchy et al., 2007; Prasad et al., 2009), provides investigators additional opportunities for mining large phospho-sites databases for ion channel phosphorylation sites.

Recent high-throughput analyses of the mouse brain phosphoproteome

Wisniewski et al. (2010) analyzed phosphosites on whole brain tissue with parallel whole protein and peptide level fractionation methods. A crude brain homogenate solubilized in detergent buffer was digested using a recently developed Filter-Assisted Sample Preparation method, rather than conventional in-solution or in-gel digestion methods (Wisniewski et al., 2009). The resultant peptides were directly subjected to protein size exclusion chromatography, or applied to anti-phosphotyrosine antibody beads. Phosphopeptides were then enriched by binding to TiO₂ beads in the presence of dihydroxybenzoic acid to avoid nonspecific binding, and/or further fractionated by strong anion exchange (SAX) chromatography. Using an LTQ-Orbitrap MS instrument, the 10 most intense precursors at a resolution of 60,000 were selected, and the precursors were fragmented through collision-induced dissociation (CID), one of the most widely used peptide fragmentation methods. Peptide identification is accomplished by matching the acquired CID mass information with a segment of the sequence from a protein database. For all of the CID tandem mass spectra, the MASCOT search engine was used to search a mouse protein sequence database (i.e., mouse IPI database, version 3.46). Note that such large-scale peptide and protein identification approaches often contain nonspecific matching with a false segment of protein sequence, resulting in incorrect peptide identification. To assess the identification in large-scale data, a modified protein sequence database was applied, which contains forward (real) and reverse (virtual) protein sequences (total \sim 110,572 entries). A false-positive rate was calculated, based on the proportion of incorrect identifications assigned to reverse sequences relative to the total identifications (forward and reverse databases). In this study, false-positive rates for both peptides and proteins were 1%. The search yielded 12,035 unique phosphosites on 4,579 proteins, including 231 different phosphosites on 42 different voltage-gated ion channel α subunits, as detailed in Table I.

Trinidad et al. (2008) analyzed phosphosites on postsynaptic density fractions generated from four different mouse brain regions by differential centrifugation and sucrose gradient density centrifugation. After in-solution digestions, the digested peptide samples from cortex, midbrain, cerebellum, and hippocampus were individually labeled with four different iTRAQ reagents (114, 115, 116, and 117 D, respectively), to allow for the subsequent identification of peptides originating from the different brain regions. A mixture with equal amounts of each sample was subjected to strong cation exchange (SCX) chromatography, which yielded over 90 fractions. Binding to TiO₂ beads further enriched the phosphopeptides. Eluted phosphopeptides were analyzed on a hybrid quadrupole time-of-flight MS (QSTAR Pulsar) instrument. All CID tandem mass spectra were searched by Analyst QS software against a Uniprot Mus musculus database containing original and randomized protein sequences (64,717 entries). Phosphopeptide identification and site assignment was manually performed with diagnostic peaks (e.g., high abundant neutral loss peak) when appropriate, and quantification of iTRAQ-labeled phosphopeptides was performed using "Proteinprospector" software. The false-positive rate was 0.12%. This study yielded 1,564 unique phosphosites on 831 proteins, including 52 different phosphosites on 19 different voltage-gated ion channel α subunits (Table I).

Munton et al. (2007) analyzed phosphosites on naive and stimulated mouse brain synaptosomes. Tryptic peptides generated by in-solution digestion were subjected to SCX chromatography, and five of the SCX fractions were further enriched by immobilized metal ion chromatography (IMAC). Eluted material was analyzed on MALDI TOF-TOF MS, ion trap LCQ, and LTQ-FT MS instruments with a reject mass list for common air contaminants. All CID tandem mass spectra from these synaptosomal phosphoproteomes were searched using Mascot against an EBI mouse protein database (32,849 entries). The false-positive rate was not reported. This study yielded 974 unique phosphosites on 499 proteins, including 32 different phosphosites on 16 different voltage-gated ion channel α subunits (Table I).

Tweedie-Cullen et al., (2009) analyzed phosphosites on a synaptic fraction prepared by differential centrifugation and sucrose gradient density centrifugation. Isolated nuclear, synaptic, and histone proteins were digested in solution, and the resultant tryptic peptides were subjected to SCX chromatography, and the early

eluting phosphopeptide-rich fractions applied to TiO₂ or IMAC beads. Eluted phosphopeptide samples were analyzed by three different types of MS instruments: MALDI TOF/TOF, LTQ-FT, or LTQ-Orbitrap. In the case of the mass analysis with the LTQ-Orbitrap instrument, lock mass was used to increase mass accuracy. Database analysis of the total CID tandem mass spectra was performed against an EBI mouse protein database (42,656 entries). The false-positive rate was 0.53%. All assigned tandem spectra with phosphorylation modifications were manually inspected and filtered out with strict criteria (MASCOT expected value below 0.05). Normalized delta ion scores were calculated with scores between two top ranking peptides and used for precise site assignment (<0.4). This study yielded 1,341 unique phosphosites on 638 proteins, including 32 different phosphosites on 14 different voltage-gated ion channel α subunits (Table I).

While the phosphosites identified in the above studies were confirmed using the most strict proteomic criteria and manual inspections, the bulk of the phosphosites obtained from these high-throughput approaches were not experimentally validated by other means. Recent proteomic technological innovations using MS have lead to a wealth of newly identified phosphosites on cellular proteins but, to date, there exist few alternative approaches to effectively cross-validate phosphosite identification. Therefore, the current method of determining the falsepositive rate of these high-throughput data are based entirely on the dataset from that particular mass spectrometric analysis, and not any independent evaluation. This may not be sufficient for data validation of all phosphosites. For example, a recent study of the yeast phosphoproteome showed that applying a single false discovery rate for all peptide identifications significantly overestimates the occurrence of rare modifications such as tyrosine phosphorylation (there are no dedicated tyrosine kinases in yeast) (Gnad et al., 2009). An appropriate false discovery rate threshold confined to phosphopeptides, among all peptides identified, is adjustable for more sensitive or more reliable data analysis. Whether the identified phosphosites are located in structurally accessible protein regions may be a further consideration when determining false positives; this is rarely an option for ion channel α subunits, for which few structures are available, and those that are (e.g., Kv1.2; Long et al., 2005) lack the cytoplasmic domains targeted by phosphorylation. Effective validation of the biological role of any identified phosphosites still involves using biochemical, cell biological, and electrophysiological analyses of individual proteins expressing site-specific mutations in the identified phosphosites.

Analysis of the obtained datasets for ion channel phosphosites

An overview of the dataset (Table I) focusing on the location of the identified phosphosites on the 24 transmembrane segment ion channel α subunits reveals that

 $\label{eq:table} \texttt{TABLE} \ \mid \\ \textit{Phosphorylation sites identified on voltage-gated ion channel} \ \alpha \ \textit{subunits}$

N-term S15 S15 SCN2A N-term S20 ID I-II S468	Subunit/ location	Study/accession no./site	Study/accession no./site	Study/ accession no./site	Study/ accession no./site	Subunit/ location	Study/accession no./site	Study/accession no./site	Study/ accession no./site	Study/ accession no./site
Dilling S845	Cav1.2/	W:Q0PCR6-1	Tr: Q01815	M: Q0PCR6-		ID I-II	S428			
Carell	CACNA1C			1		ID I-II	T441	T441		
CACCAINA Tr. 197445 Tr. 19745 Mr. 19746 Tr. 19745 DI IIII S.793 S.793 S.793 S.795 DI IIII S.795 S.856 S.856 S.856 S.856 S.856 DI IIII S.795 S.795 S.795 DI IIII S.795 S.795 DI IIII S.795 S.795 DI IIIII S.795 S.795 S.795 DI IIII S.896 S.896 S.896 S.896 DI IIII S.795 S.795 DI IIII S.896 S.896 S.896 S.896 DI IIII S.896 S.896 S.896 S.896 DI IIII S.896 S.896 S.896 S.896 DI IIII S.897 DI IIIII S.897 DI IIII S.897 DI IIII S.896	ID II-III	S845		S845		ID II-III	S737	S737	S737	S737
DI-HI	C-term	S1721	S1691			ID II-III	S740	S740		
Die		W: P97445	Tr: P97445	M: P97445	T:P97445			S746		
10 11 11 14 14 18 18 18 18	ID I-II	T411								
Dilling S722	ID I-II	S468						\$856	\$856	
Di Hall S755	ID II-III	S752	S752		S752		3630		5050	
D1 HII	ID II-III	S755	S755		S755		\$866	1003		
Di Hill S867	ID II-III				S792					
Dil-III	ID II-III	S867								
Circle	ID II-III	S1038	S1038					\$1051		
Catern	C-term	T1935					31031			
Cterm	C-term	S1946					T1004	31030		
Cacers	C-term	T1948						\$9054		
Catern	C-term			S1981	S1981			32034		
Catern	C-term			Y2027					C9079	
Catern	C-term		S2028				32073			
Catern	C-term		S2030				W. OFFIET	T OFCITE	52097	T. OFFIRE
Catern	C-term	S2068					W: Q55UF7	1r: Q55UF5		1: Q55UF5
Catern	C-term	T2070					\$467	\$466 /\$467		\$467
Caterm \$2078 ID II-III \$1149 Caterm \$2091 \$2991 ID II-III \$1171 Caterm \$2220 \$2220 \$2220 ID II-III \$1172 Caterm \$2252 \$2241/T2244/ Caterm \$2889 Caterm \$2889 Caterm \$2273 \$2273 Caterm \$2273 Caterm \$2273 Caterm \$23239 Caterm \$2288 Caterm \$2281 Caterm \$23293 Caterm \$2283 Caterm \$2281 Caterm \$23293 Caterm \$2281 Caterm \$2281 Caterm \$23293 Caterm \$2281 Caterm \$2281 Caterm \$23293 Caterm \$2281 Caterm \$2281 Caterm \$2324 Tr. A2AIR* Caterm \$2361 Di Hi \$446 \$745 \$745 DI HiIII \$948 Di HiII \$745 \$749 \$740 \$740 \$740 <td>C-term</td> <td>S2071</td> <td></td> <td></td> <td></td> <td></td> <td>3407</td> <td></td> <td></td> <td>3407</td>	C-term	S2071					3407			3407
Cerem \$2091 \$2090 \$2220 \$2220 \$10 H-III \$1172 Cerem \$2252 \$2241/\$T2244/\$ S2250/\$\$2252 Cerem \$2089 Cerem \$2252 \$2250/\$\$52252 Cerem \$2145 Cerem \$22303 \$2273 Cerem \$22273 Cerem \$2281 Cerem \$2281 Cerem \$2283 Cerem \$2281 Cerem \$2283 Cerem \$2281 Cerem \$2283 Cerem \$2281 Cerem \$2283 Cerem \$2283 Cerem \$2283 Cerem \$2281 Cerem \$2281 Cerem \$2281 Cerem \$2281 Cerem \$2281 Cerem \$2283 Cerem \$2281 DI-III \$446 DI-IIII \$948 DI-IIII \$748 \$745 \$745 DI-IIII \$948 DI-IIII \$753 \$784 \$783 \$783 DI-III	C-term	S2078								
Cetem \$2200 \$2200 ID II-III \$1172 Ceterm \$2255 \$2250 \ \$2255 Ceterm \$2089 Ceterm \$2273 \$2273 Ceterm \$2281 Ceterm \$2303 \$2303 Ceterm \$2281 Ceterm \$2329 Ceterm \$2281 Cave.2./ W: 055017 Tr. A2AIR7 M: A2AIR9 Tr. A2AIR9 Ceterm \$2283 Cave.2.// W: 055017 Tr. A2AIR7 M: A2AIR9 Tr. A2AIR9 Ceterm \$2283 CACNAII S424 Ceterm \$2361 Ceterm \$2281 ID I-II \$446 Tr. A2AIR9 Tr. A2AIR9 Oli HIII \$948 ID I-III \$446 \$745 \$745 ID II-III \$948 Tr. A2APX6 ID I-III \$748 \$749 Part III \$941 \$948 Tr. A2APX6 ID I-III \$753 \$745 \$745 ID I-III \$941 \$942 \$942 \$941 \$942 \$942 \$942	C-term	S2091	S2091				\$1171	31143		
Cerm \$2252 T2241/T2244/ \$2250/\$82255 Cerm \$2145 Cerm \$2273 \$2273 Cerm \$2273 Cerm \$2303 \$2303 Cerm \$22281 Cav2.2/ W: O55017 Tr. A2AIR7 M: A2AIR9 T: A2AIR9 Cerm \$2283 Cav2.2/ W: O55017 Tr. A2AIR7 M: A2AIR9 T: A2AIR9 Cerm \$2283 Cav2.8/CACNAIB Till S424 Cerm \$2361 F. Cerm \$2361 Di Hill \$446 F. A2AIR9 Tr. A2AIR9 Cerm \$2361 Di Hill \$446 F. A2AIR9 F. A2AIR9 F. A2AIR9 Di Hill \$446 F. A2AIR9 F. A2AIR9 F. A2AIR9 Di Hill \$745 \$745 \$745 DI Hill \$951 F. A2APX6 Di Hill \$783 \$783 \$783 DI Hill \$467 F. A2APX6 Di Hill \$892 F. A2APX6 DI Hill \$467 DI Hill \$565 Di Hill	C-term	S2200		S2220	S2220					
C-term S2273 S2273 S2273 S2273 S2273 C-term S2273 C-term S2303 S2303 C-term S2281 C-term S2281 C-term S2281 C-term S2281 C-term S2283 C-term S2283 C-term S2283 C-term S2283 C-term S2283 C-term S2283 C-term S2361 C-term S2464 S746 S745 S745 S745 ID II-III S948 ID II-III S948 S749 S745 S745 S745 ID II-III S951 S561 S565 S561 S565 S561 S565 S	C-term	S2252				C-term	S2089			
C-term S2303 S2303 S2303 C-term S2283 C-term S2283 C-term S2283 C-term S2283 C-term S2283 C-term S2283 C-term S2281 C-term S2361 C-ter	C-term	S2273			S2273					
Caterin S2329 Care S2283 Care S2281 Care S2914 S2283 S745 S74										
Cave. W: O55017										
CACNAIB			Tr: A2AIR7	M: A2AIR9	T: A2AIR9					
ID 1-11										
ID						CACNA1I	001037773.1			
ID			\$746	S745	S745					
ID				0.10	0.10					
ID II-III							W: A2APX8	Tr: A2APX6		
ID II- II			S784	S783	S783		TACE			
ID II II II S915				- /						
ID II-III										
C-term S1951 S1927 ID I-II S607							5551	CECE		
C-term S1951					S1927		960h	5000		
C-term S2014 ID I-II T721		S1951								
C-term S2221										
C-term S2244 S2245 S2242 S2242 ID I-II S730 Cav2.3/ W: IPI00331064 Tr: O88405 M: Q61290 T: Q61290 C-term S1928 CACNAIE Nav1.2/ W: B1AWN6 Tr: A2AJZ2 T: B1AWN N-term S15 S15 SCN2A N-term S20 ID I-II S468										
Cav2.3/ W: IPI00331064 Tr: O88405 M: Q61290 T: Q61290 Cerm S1928 CACNAIE Nav1.2/ W: B1AWN6 Tr: A2AJZ2 T: B1AWN N-term S15 S15 SCN2A N-term S20 ID I-II S468			S2245	S2242	S2242					
Navl.2/ W: BIAWN6 Tr: A2AJZ2 T: BIAWN N-term S15 S15 SCN2A N-term S20 ID I-II S468	Cav2.3/					C-term				
N-term S20 ID I-II S468		S15	S15				W: B1AWN6	Tr: A2AJZ2		T: B1AWN6
ID I-II 5400							\$468			
	N-term		T29	T29		117 1-11	5400			

TABLE | (Continued)

				IABLE I	(Continued)				
Subunit/ location	Study/accession no./site	Study/accession no./site	Study/ accession	Study/ accession	Subunit/ location	Study/accession no./site	Study/accession no./site	Study/ accession	Study/ accession
			no./site	no./site			20.10	no./site	no./site
ID I-II	S471				C-term	S842	S842	1. OOOBO.	S842
ID I-II	S475				HCN3	W: O88705	Tr:O88705	M: O88705	
ID I-II	S484				C-term	S633	S633	S633	
ID I-II	S486				C-term	S720			
ID I-II	S488				C-term	S936		M 070707	
ID I-II	S526				HCN4	W: O70507		M: O70507	
ID I-II	S528	07.10		Q# 40	N-term	S139		0001	
ID I-II	055.4	S540		S540	C-term	TIT TD100100710		S921	
ID I-II	S554					W: IPI00133719			
ID I-II	S558				N-term	S23		M DC0141	T. DC0141
ID I-II	S561	07.00			Kv1.2/KCNA2	W: P63141			T: P63141
ID I-II	or to	S568			C-term			T421	
ID I-II	S573				C-term	0.40.4		T433	0.40.4
ID I-II	S576	OK HO		050	C-term	S434			S434
ID I-II	0010	S579		S579	C-term	S440			0.4.41
ID I-II	S610				C-term	S441			S441
ID I-II	S623				C-term	S447	T. OCCDEO	M. OC1499	
ID I-II	S626				Kv1.4/KCNA4	•	Tr:Q8CBF8	M: Q61423	
ID I-II	T713				N-term	S101			
ID I-II	T715				N-term	S113	C100	0100	
ID I-II	S722				N-term	S122	S122	S122	
C-term	T1944				Kv1.5/KCNA5	•			
Nav1.6/ SCN8A	W:Q9WTU3				C-term	S535		M. OC1099	
ID I-II	S504				Kv1.6/KCNA6 N-term	•		M: Q61923	
ID I-II	S518					S6 T8		Т8	
ID I-II	S520				N-term Kv2.1/KCNB1		TR: Q03717	M: Q8K0D1	T. OSKADI
ID I-II	S522				N-term	W. QORODI	1K. Q03717	S12	1. Qokubi
ID I-II	S600				N-term		S15	314	
Nav1.9/	W: Q62205				C-term	S444	313		
SCN9A	201100				C-term	S484			
ID I-II	S502				C-term	S517			
ID I-II	S504				C-term	S517			
C-term	S1062				C-term	S519			
C-term	S1064				C-term	S520			
HCN1	W: O88704	Tr: O88704	M:O88704		C-term	S567			
N-term	T39	T39	T39		C-term	S655	S655	S655	S655
N-term	S69		S69		C-term	S782	3033	5055	5055
C-term	S588				C-term	T803			T803
HCN2	W:O88703	Tr: O88703	M: O88703	T: O88703	C-term	S804			S804
N-term	S90			S90	Kv2.2/KCNB2				3001
N-term	S119	S119	S119		C-term	T478			
N-term	S131				C-term	S481			
N-term	S134				C-term	S488			
C-term	S726				C-term	S490			
C-term		S743			C-term	S503			
C-term			S750		C-term	S507			
C-term	S756				C-term C-term	S530			
C-term	S757				Kv3.1/KCNC1		Tr: Q3TR92		T: P15388
						W: I 13300	11: Q31K94		1:113368
C-term		S771	S771				-		
	S795	S771	S771		N-term	S158	-		Q160
C-term C-term C-term	S795 S834	S771	S771				T421		S160

TABLE I (Continued)

				IABLE I	(Continuea)				
Subunit/	Study/accession	Study/accession	Study/	Study/	Subunit/	Study/accession	Study/accession	Study/	Study/
location	no./site	no./site	accession no./site	accession no./site	location	no./site	no./site	accession no./site	accession no./site
C-term	S468				Kv7.5/	W: Q9JK45			
C-term	T483				KCNQ5				
Kv3.2/KCNC2	W: P70311				C-term	S469			
C-term	S509				C-term	S477			
C-term	S557				Kv10.1/	W: Q32MR7			
C-term	S604				KCNH1				
C-term	S619				C-term	S899			
Kv3.3/KCNC3	W: Q63959	Tr: Q63959			C-term	S904			
C-term	S717	S717			Kv10.2/ KCNH2	W: XP_ 001477398.1	Tr: 035219		
C-term	S732				N-term	S281			
C-term	S740				N-term		S320/T321/S322		
C-term	T751				N-term	S362			
C-term	S755				N-term	S364			
Kv3.4/KCNC4	•				C-term	S913			
C-term	S555				C-term	S916			
Kv4.1/KCND1	W: Q03719				C-term	S1180			
C-term	S460				Kv10.5/	W: Q920E3			
C-term	S555				KCNH5	W. Q32023			
Kv4.2/KCND2	W: Q9Z0V2		M: Q9Z0V2	T: Q9Z0V2	C-term	S883			
N-term	T154				C-term	S888			
C-term	S548		S548		Kv10.7/	W: A2AUY8			
C-term	S552			S552	KCNH7				
Kv4.3/KCND3	W: Q9Z0V1				N-term	S174			
N-term	S153				N-term	T318			
Kv5.1/KCNF1	W: Q7TSH7				N-term	S319			
C-term	S444				C-term	S891			
C-term	S470				C-term	S1007			
C-term	S472				C-term	S1135			
Kv7.2/	W: NP_034741	Tr: NP_034741	M: NP_	T: NP_	C-term	S1169			
KCNQ2			034741	034741	C-term	S1174			
N-term	S52				C-term	S1188			
C-term	S352			S352	Slo1/	W: Q08460-1	Tr: Q08460-1	M: Q08460-1	T: O08460-1
C-term	S457				KCNMA1	,,, 2001001	111 200 100 1	111 2001001	1. 2001001
C-term	T462				N-term			S136	
C-term	S466		S466		C-term	T709	T709		
C-term	S468		S468		C-term	S711	S711	S711	S711
C-term	S476				C-term	S923			S923
C-term				S485	C-term	S924			S924
C-term	S507	S507			C-term	5021			S928
C-term	Y671				C-term	S938			
C-term	S673	S673			C-term	5556	S1060		
C-term	T728				C-term	T1061	T1061	T1061	T1061
C-term	S729				C-term	T1064	11001	11001	11001
C-term	S799				TrpC3/	W:B1ATV3-1			
C-term	S801				TRPC3	W.BIAI V3-1			
Kv7.3/	W: Q8K3F6	Tr: Q14B66	M: Q8K3F6		C-term	S807			
KCNQ3	-	-	-		TrpC6/	W: Q61143			
N-term	T82				TRPC6	Xu1113			
C-term	S579				C-term	S814			
C-term	T580	T577			TrpM2/	W: Q91YD4			
C-term	S596				TRPM2	-			
C term	5550				IKPMZ				

TABLE I (Continued)

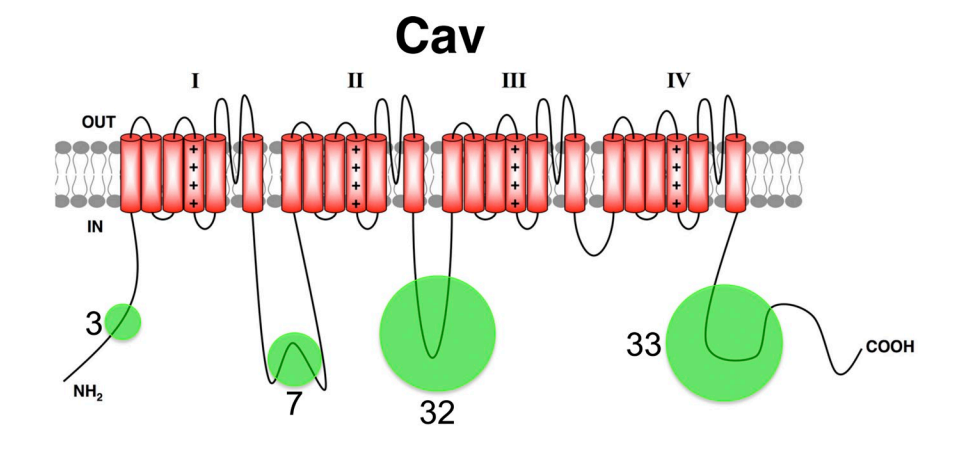
		(
Subunit/ location	Study/accession no./site	Study/accession no./site	Study/ accession no./site	Study/ accession no./site
TrpM3/ TRPM3	W: Q5F4S9	Tr: Q5F4S9		
C-term	T1299			
C-term	S1301			
C-term	S1314			
C-term	S1317			
C-term		T1336/S1338/ T1340/S1341		
C-term	S1605			
C-term	S1608			
C-term	S1609			
TrpV2/ TRPV2	W: Q9WTR1			
N-term	T14			
N-term	S15			

Note additional sites identified on Slo1/KCNMA1 Q08460-2: T670 (W) and S672 (W, T), corresponding to T709 and S711 in Q08460-1. W, Wisniewski et al., 2010; Tr, Trinidad et al., 2008; M, Munton et al., 2007; T, Tweedie-Cullen et al., 2009.

for Cav channel α subunits, phosphorylation is primarily split between the ID II-III linker and the C terminus (Fig. 1), whereas for Nav channel α subunits, phosphory-

lation is primarily (90%) on the ID I-II linker (Fig. 1), as suggested by previous studies (Cantrell and Catterall, 2001). All of the six transmembrane ion channel α subunits (Fig. 2) have the majority of their phosphosites on the C terminus, although this varies from $\approx 90\%$ for Kv7 and Slo1-BK channel family members, to $\approx 65\%$ for Kv10 and HCN family members.

An overall number of unique phosphosites identified shows that the largest ion channel α subunits, namely those within the 24 transmembrane segment family of Cav and Nav channel α subunits, have the most extensive phosphorylation, with Cav2.1 (24 phosphosites), Nav1.2 (23 phosphosites), and Cav2.3 (22 phosphosites) topping the list (Table I). This may be expected given the large size of these polypeptides (2,000–2,400 amino acids) and that only one α subunit is present per channel complex. Among the six transmembrane segment family members, which are smaller polypeptides and assemble as tetramers in the final channel complex, Kv7.2 (15 phosphosites), HCN2 (14 phosphosites), Kv2.1 (13 phosphosites), and Slo1-BK (10 phosphosites) are notable in their extensive representation, suggesting a high degree of phosphorylation-dependent modulation of these channels. Note that while these data suggest extensive multisite phosphorylation exists



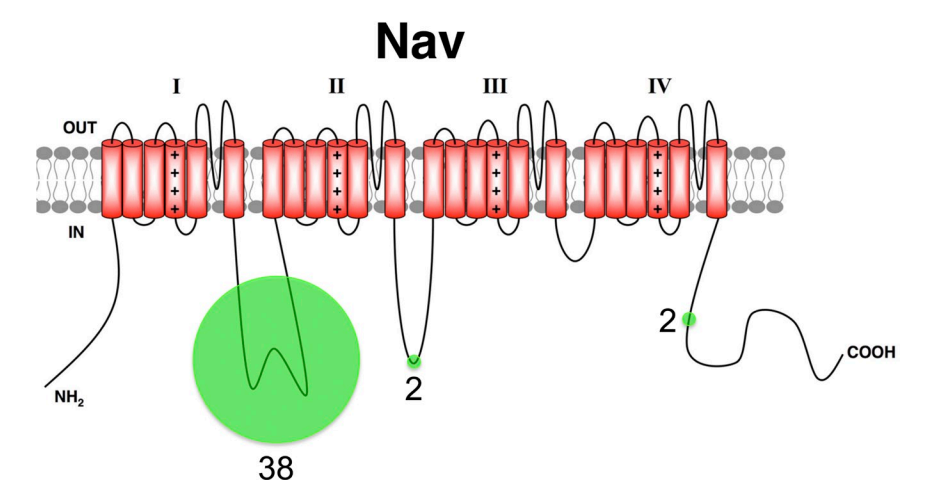


Figure 1. Schematic of phosphosites identified in high-throughput studies on 24 transmembrane segment ion channel α subunits. Areas of the green circles represent the percentage of phosphosites found within a specific cytoplasmic domain (N-terminal, ID I-II, ID-II-III, or C-terminal). Numbers adjacent to circles represent the total number of unique phosphosites identified within that domain for all members of that family (Cav: six members; Nav: four members).

on individual molecules of ion channel α subunits, these studies have not provided conclusive data as these phosphosites come from relatively small tryptic fragments of the larger polypeptides. As such, except for the small subset of neighboring phosphosites found within the same multiply phosphorylated tryptic peptide, it is formally possible that the multiple phosphosites identified in these ion channel α subunits are stochastically distributed in different molecules.

Note that representation on the list of "most phosphorylated" ion channel α subunits is likely a combination of not only the actual extent of phosphorylation, but also

nature of the phosphorylation, as the techniques employed (MS-based analyses of tryptic peptides) bias the analysis toward phosphosites on tryptic peptides with a chemical nature (e.g., size, charge, hydropathy, etc.) that makes them amenable to detection by mass spectrometers. Of course, the overall abundance of a specific ion channel α subunit in a given sample, whether it is whole brain or a subcellular fraction thereof, will also affect its representation in samples with high proteomic and phosphoproteomic complexity, such as those used for global analyses. As such, enriching for ion channel α subunits is an attractive approach to increase coverage of their phosphoproteome.

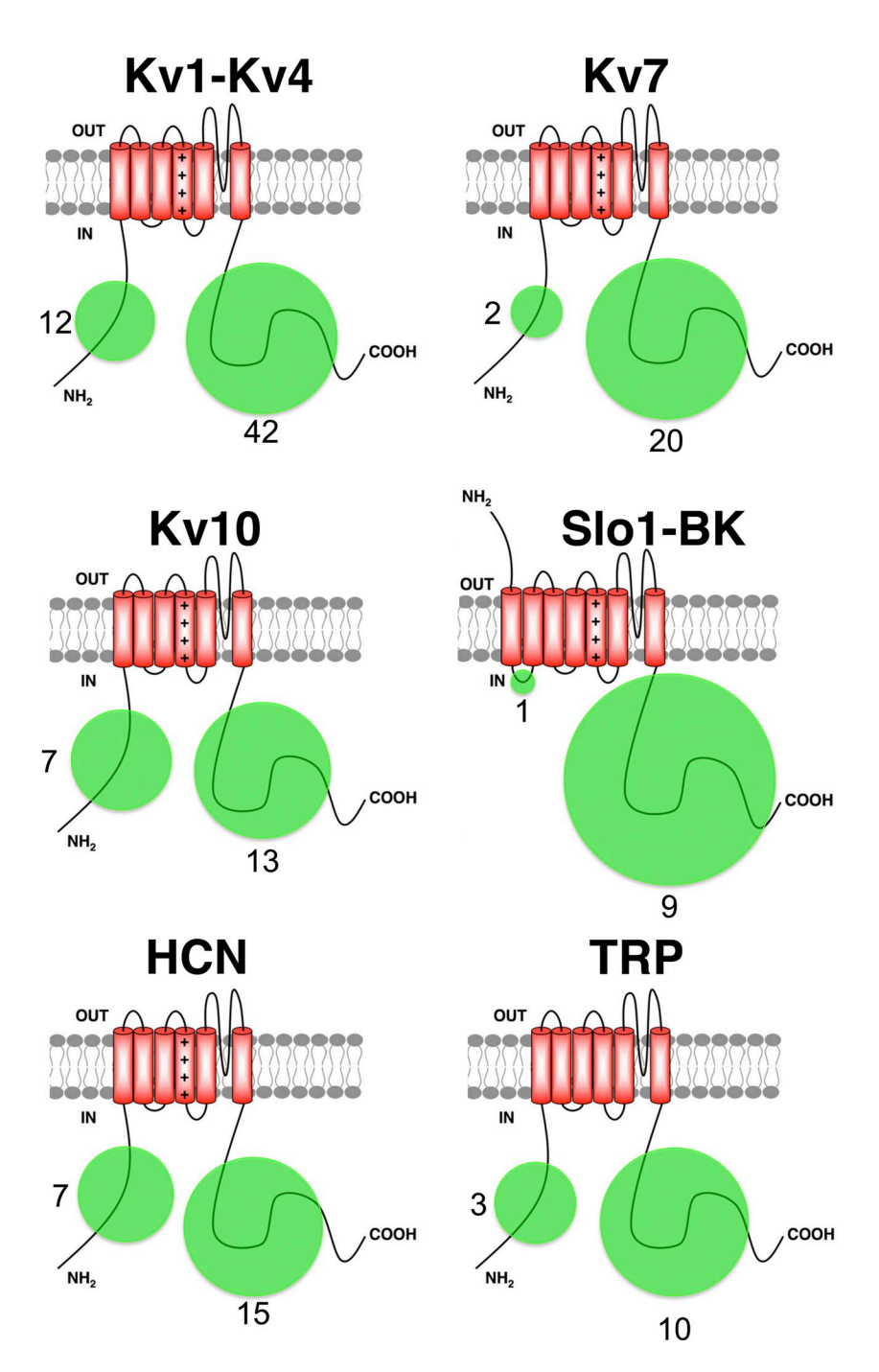


Figure 2. Schematic of phosphosites identified in high-throughput studies on six transmembrane segment ion channel α subunits. Areas of the green circles represent the percentage of phosphosites found within a specific cytoplasmic domain (N or C terminus). Numbers adjacent to circles represent the total number of unique phosphosites identified within that domain for all members of that family (Kv1-4: 14 members; Kv7: 3 members; Kv10: 4 members; Slo1-BK: 1 member; HCN: 4 members; TRP: 5 members).

These high-throughput approaches focused exclusively on adult mouse brain. This raises questions as to the implications for the rat and human brain orthologues of these mouse brain ion channel α subunits. If conservation of the phosphoacceptor site itself is any indication, then these mouse brain data are likely to have strong implications for studies in other mammals. Focusing on the ion channel α subunits within a subfamily that exhibit the highest number of identified phosphosites (Cav2.1, Nav1.2, Kv2.1, Kv7.2, and TRPM3), we found that, with the exception of mouse and human Cav2.1 (87% overall identity), overall sequence identity between mouse, rat, and human ion channel α subunit orthologues was 93% or higher. As to the phosphosites themselves (85 in total), there was 100% conservation of every site in mouse, rat, and human Nav1.2 (23 phosphosites), Kv2.1 (13 phosphosites), Kv7.2 (15 phosphosites), and TrpM3 (8 phosphosites), and for human Cav2.1, 92% conservation (22/24). It should be noted that conservation of the phospho-acceptor site itself may not in itself suggest that the site is phosphorylated, as changes in neighboring amino acids in the primary, secondary, or tertiary structure may alter protein kinase consensus motifs (Ubersax and Ferrell, 2007). Also note that with the exception of the study by Munton et al., these studies focused on samples prepared from animals under basal conditions, and may not contain examples of sites whose phosphorylation requires specific stimuli.

Functional implication of phosphosites identified in high-throughput approaches

There are numerous examples of phosphorylation at defined sites on specific ion channels dynamically regulating how these ion channels impact cell function. One way that phosphorylation can act is through altering the abundance of specific ion channels in specific membrane domains. This can occur via changes in the proportion of ion channels in intracellular membranes versus the plasma membrane, by impacting the rates of channel exocytosis and endocytosis, or by affecting the density of channels in a specific plasma membrane subdomain via effects on channel clustering. Phosphorylation can also affect the gating of ion channels, altering the probability that an ion channel will be open under a given set of conditions.

A large literature exists providing a large number of examples of stimuli impacting ion channel abundance, distribution, and gating. As many of these stimuli are known to act through signaling pathways leading to activation of protein kinases or protein phosphatases, the assumption has been that the effects are meditated through changes in the phosphorylation state of the ion channel subunits themselves. In some cases, regulation can be obtained for recombinant ion channels expressed in heterologous cells, in which case candidate

phosphosites can be identified using phosphosite prediction software (e.g., http://www.cbs.dtu.dk/services/ NetPhosK/; http://scansite.mit.edu/motifscan_seq .phtml; http://www.hprd.org/PhosphoMotif_finder), and mutations generated that lock specific candidate phosphosites in either a dephospho- or phospho-mimetic state (e. g., Ser to Ala or Asp mutations, respectively). Data obtained from these approaches have allowed for the identification of specific sites critical to phosphorylation-dependent modulation of channel abundance, distribution, or function. However, rarely have these studies directly shown that the impact of the mutations is via altering phosphorylation state, and that the mutation only altered phosphorylation at the mutated site. Moreover, there are few cases where the candidate phosphosite being studied is known to be modified by phosphorylation in native cells. As such, we are left with a large number of candidate phosphosites whose mutation impacts the channel, but whose physiological relevance is unknown.

The recent high-throughput approaches described here have yielded, for the most part, a dataset completely complementary to these types of studies, in providing a large amount of information as to which sites are found phosphorylated in native cells, but without any functional insights. In a few cases, which we detail below, phosphosites identified in these recent phosphoproteomics studies have provided in vivo relevance to studies already performed in heterologous cells. Future studies aimed at determining the functional impact of the phosphosites we highlight here will serve to increase the number of examples of phosphosites that appear in vivo, and functional relevance is known.

Phosphorylation of Cav2.2 α_1 subunits, which regulate neurotransmitter release from nerve terminals, in their DI-DII linker region has been proposed to play a crucial role in diverse aspects of Cav channel function. For example, mutation of rat Cav2.2 at the site identified in mouse brain (using accession no. O55017) as S424 mediates PKC-dependent Cav2.2 inhibition (Fang et al., 2006; Rajagopal et al., 2009). ERK-dependent upregulation of Cav2.2 channels is mediated through phosphorylation of the site identified in mouse brain as S446 (Martin et al., 2006). In the DII-DIII linker, PKC phosphorylates the sites identified in mouse brain as S773 and S892, and CaMKII at S783, and impacts syntaxin1A-Cav2.2 interaction (Yokoyama et al., 2005). PKC-dependent phosphorylation on S892 was also found to disrupt interaction with syntaxin 1A and abolish the hyperpolarizing shift in the steady-state inactivation caused by this protein-protein interaction (Jarvis and Zamponi, 2001).

The predominant sodium channel in brain, Nav1.2, is a substrate for PKA phosphorylation in its DI-DII linker domain (Cantrell et al., 1997; Smith and Goldin, 1997). PKA phosphorylates Nav1.2 at the in vivo mouse brain sites S573, S610, and S623, calcineurin dephosphory-lates these three phosphosites, and protein phosphatase 2A (PP2A) dephosphorylates S610 (Smith and Goldin, 1997). PKA causes a decrease of the Nav peak current triggered by dopaminergic stimulation of rat hippocampal neurons, but does not alter the voltage dependence or kinetic parameters. The S573A mutation abolishes the dopamine-induced PKA effects (Cantrell et al., 1997).

Kv1.2 channel subunits are expressed in axons and nerve terminals, and modulate action potential propagation and nerve terminal excitation. Site-directed mutagenesis studies showed that the S440A and S441A mutations diminish Kv1.2 surface expression and whole cell current (Yang et al., 2007). The S449A substitution causes a decrease in phosphorylation at S440 and S441, again leading to diminished surface expression (Yang et al., 2007). PKA phosphorylates Kv1.2 at S449 (Johnson et al., 2009).

Kv2.1 is expressed in large clusters in the somatodendritic membrane of most neurons (Trimmer, 1991). Kv2.1 is extensively phosphorylated in vivo, and increased neuronal excitability leads to calcineurin-mediated Kv2.1 dephosphorylation, a loss of clustering, and hyperpolarizing shifts in voltage-dependent gating (Misonou et al., 2004, 2005, 2006). A mass spectrometrybased analysis of Kv2.1 purified from rat brain identified 16 phosphosites (Park et al., 2006; Mohapatra et al., 2007), of which five (S15, S484, S520, S567, S655, and S804) were also identified in high-throughput approaches detailed here (Table I). Of the phosphosites identified in the high throughput studies, mutations at S15, S567, and S655 partially mimic and occlude the effects of dephosphorylation in causing hyperpolarizing shifts in the voltage-dependent gating. In addition, phosphorylation on S804 via p38MAPK increases the surface expression of Kv2.1, leading to neuronal apoptosis (Redman et al., 2007).

Ky channels containing Ky4.2 α subunits mediate transient A-type K⁺ currents in neurons, which are critically involved in the regulation of dendritic excitability and plasticity (Shah et al., 2010). In hippocampal slices, PKA activation by forskolin and other pharmacological agents results in Kv4.2 phosphorylation at S552 (Anderson et al., 2000). PKA-dependent phosphorylation of this residue results in a depolarizing shift of Kv4.2 activation, but only in presence of the auxiliary subunit KChIP3 (Schrader et al., 2002). PKA phosphorylation at S552 also mediates AMPA-stimulated Kv4.2 internalization from dendritic spines (Hammond et al., 2008). Note that a previous mass spectrometry-based analysis of Kv4.2 purified from rat brain (Seikel and Trimmer, 2009) identified four phosphosites (S548, S552, S572, and S575) of which two (S548 and S552) were found in the high-throughput analyses of mouse brain (Table I).

Kv7 (KCNQ) subunits form neuronal Kv channels that underlie the M-current (so-called due to its modulation

by muscarinic signaling). These channels localize in axon initial segments, nodes of Ranvier, and somata throughout the nervous system. Of the residues found phosphorylated in mouse brain (Table I), PKA phosphorylation of KCNQ2 at S52 has been shown to enhance KCNQ2 currents in heterologous cells (Schroeder et al., 1998). A previous mass spectrometric–based analysis identified phosphorylation at either S578 or T579 on recombinant human KCNQ3 expressed in heterologous cells (Surti et al., 2005). Mutations at these positions in KCNQ3 eliminate functional expression of KCNQ2/3 channels (Surti et al., 2005). These sites are analogous to in vivo phosphosites identified in mouse brain proteomic studies on Kv7.3 at S579 and T580.

Large conductance Ca²⁺-activated K⁺ (Slo1-BK) channels are involved in neuronal repolarization and rapid afterhyperpolarization. PKC-dependent phosphorylation on S695 of the bovine Slo1-BK α subunit (corresponding to S711 of the mouse isoform shown in Table I) decreases the open probability of the channel, an effect countered by protein phosphatase 1 (Zhou et al., 2010). PKG-dependent phosphorylation on S855 together with S869 (S869 corresponding to S924 in the mouse isoform used here) enhances the current amplitude of the human Slo1-BK channel in *Xenopus* oocytes (Nara et al., 2000).

The overall nature of ion channel phosphorylation revealed by high-throughput analyses

To gain insights into whether these data provide insights into the predominance of ion channel phosphorylation by a particular protein kinase, we have analyzed the phosphosites on the ion channel α subunits with the most extensive phosphorylation (Cav2.1, Nav1.2, Kv2.1, Kv7.2, and TRPM3) for consensus motifs using NetPhosK (http://www.cbs.dtu.dk/services/NetPhosK/). Of the 83 phosphosites analyzed, the most predominant motifs recognized were for the proline-directed protein kinases p38MAP kinase, GSK3 and Cdk5, with 30 phosphosites being scored for phosphorylation by one or more of these protein kinases. There were 13 phosphosites that scored as consensus motifs for PKA, and 10 for PKC. There were 19 phosphosites that did not score as sites for any consensus protein kinase motif. These results are somewhat consistent with our previous analyses of phosphosites found on Nav1.2 (Berendt et al., 2010) and Kv2.1 (Park et al., 2006) purified from rat brain, which revealed a predominance of phosphosites for proline-directed protein kinases, as well as several sites not recognized by any prediction program.

In this regard it is interesting to compare the data obtained from these high throughput global analyses versus those from studies on purified ion channel α subunits (Table II). Recent studies from our laboratory have used this approach for Nav1.2 (Berendt et al., 2010), Kv2.1 (Park et al., 2006), and Slo1-BK (in collaboration

TABLE II

Results from high versus low-throughput analyses

Results f	rom high versus low-through $_{ m I}$	put analyses				
Subunit/location	High accession no./site	Low accession no./site	Subunit/location	High accession no./site Low accession no./site		
Nav1.2/SCN2A	B1AWN6/Mus	P04775-1/rat	C-term	S567	S567	
N-term		S4	C-term		S590	
ID I-II	S468	S468	C-term		S607	
ID I-II	S471	S471	C-term	S655	S655	
ID I-II	S475		C-term		S719	
ID I-II	S484	S484	C-term		S771	
ID I-II	S486	S486	C-term	S782		
ID I-II	S488		C-term		S799	
ID I-II	S526		C-term	T803		
ID I-II	S528	S528	C-term	S804	S804	
ID I-II	S540		C-term		T836	
ID I-II	S554	S554	Slo1/KCNMA1	Q08460-1/Mus	Q62976-2/Rat	
ID I-II	S558		N-term	S136	S106	
ID I-II	S561		N-term		S107	
ID I-II	S568		C-term		S551	
ID I-II	S573		C-term	T709	T676	
ID I-II	S576		C-term	S711	S678	
ID I-II	S579	S579	C-term		S691	
ID I-II	S610	S610	C-term		T694	
ID I-II	S623	S623	C-term		S695	
ID I-II	S626		C-term		S813	
ID I-II		S687	C-term		S818	
ID I-II		S688	C-term		S879	
ID I-II	T713		C-term		T883	
ID I-II	T715		C-term	S923	S890	
ID I-II	S722	S722	C-term	S924	S891	
C-term		S1966	C-term	S928	S895	
C-term	T1944	T1944	C-term	S938	S905	
Kv2.1/KCNB1	Q8K0D1/mus	P15387/rat	C-term	S1060		
N-term	S12	,	C-term	T1061	T1001	
N-term	S15	S15	C-term	T1064		
C-term	S444		C-term		S1059	
C-term		S457	C-term		S1101	
C-term	S484		C-term		S1106	
C-term		S496	C-term		S1112	
C-term		S503	C-term		S1113	
C-term	S517		C-term		S1116	
C-term	S518		C-term		S1117	
C-term	S519		C-term		S1118	
C-term	S520	S520	C-term		S1121	
C-term		S541	C-term		S1124	
			C-term		T1125	

with Fakler et al.) (Yan et al., 2008), among others. Note that in each case, the analyses of purified ion channel α subunits were from rat brain, while the global analyses were performed on mouse brain. For Nav1.2, of the 23 phosphosites identified in these global analyses, 10 were found in the single-target analysis of purified Nav1.2 (Berendt et al., 2010). However, the MS-based analyses of purified Nav1.2 identified six phosphosites not seen in the global analyses. In the case of Kv2.1, of the 13 phosphosites identified in the global analyses of mouse brain, six were observed in the analysis of Kv2.1 purified

from rat brain, which also revealed the presence of 10 additional phosphosites not seen in the global analyses (Park et al., 2006). For Slo1-BK, of the 10 unique phosphosites identified in the global analyses, all but two were also observed in the analyses of the purified Slo1-BK, which also provided an additional 20 phosphosites (Yan et al., 2008).

These comparisons suggest that while the dataset from these global analyses represents a wealth of information for ion channel researchers, parallel approaches using enrichment of the target ion channel α subunits provide datasets that are oftentimes more extensive, revealing additional phosphosites that may play important roles in the modulation of these channels. What these datasets do suggest is that neither approach used in isolation has yet to provide a comprehensive view of phosphosites on any given ion channel α subunit. Of course, phosphorylation is by nature dynamic, such that variations in the exact state of the animal subject, details of sample preparation, and other factors that are difficult to precisely control can influence the dataset obtained. Moreover, these analyses were primarily performed on samples derived from whole adult rat or mouse brains, such that phosphosites highly represented in other temporal and spatial contexts may be underrepresented. It is also important to stress that any site identified in phosphoproteomic screens needs to be directly confirmed by at least one independent method, for example multiple reaction monitoring (which can also provide quantitative information; Rinehart et al., 2009), immunoblotting with phosphospecific antibodies (Park et al., 2006), or other approaches.

The wealth of data obtained from these studies raises the question as to whether we in the ion channel field should simply sit back and wait as these types of global analyses, being performed by our colleagues in the proteomics field, provide us with intriguing and extensive sets of in vivo phosphosites. We would argue that we should accept such bountiful gifts with gratitude and appreciation, but that we in the ion channel field need to continue our complementary efforts to identify in vivo phosphosites through focused analyses of individual ion channel subunits purified from brain and other tissues. Together, these approaches are likely to yield a comprehensive dataset that will allow for a more complete picture of the nature and extent of in vivo phosphosites crucial to dynamic regulation of native ion channel expression, localization, and function.

We thank Dr. Ry Tweedie-Cullen for providing data sets. We are grateful to Dr. Jon Sack and Ms. Ashleigh Evans for critical comments on the manuscript.

The work cited from our laboratory was supported by National Institutes of Health grants NS38343, NS42225, NS64428, and NS64957.

Angus C. Nairn served as editor.

Submitted: 8 October 2010 Accepted: 17 November 2010

REFERENCES

- Amanchy, R., B. Periaswamy, S. Mathivanan, R. Reddy, S.G. Tattikota, and A. Pandey. 2007. A curated compendium of phosphorylation motifs. *Nat. Biotechnol.* 25:285–286. doi:10.1038/nbt0307-285
- Anderson, A.E., J.P. Adams, Y. Qian, R.G. Cook, P.J. Pfaffinger, and J.D. Sweatt. 2000. Kv4.2 phosphorylation by cyclic AMP-dependent protein kinase. *J. Biol. Chem.* 275:5337–5346. doi:10.1074/jbc.275.8.5337

- Berendt, F.J., K.S. Park, and J.S. Trimmer. 2010. Multisite phosphorylation of voltage-gated sodium channel alpha subunits from rat brain. *J. Proteome Res.* 9:1976–1984. doi:10.1021/pr901171q
- Cantrell, A.R., and W.A. Catterall. 2001. Neuromodulation of Natchannels: an unexpected form of cellular plasticity. *Nat. Rev. Neurosci.* 2:397–407. doi:10.1038/35077553
- Cantrell, A.R., R.D. Smith, A.L. Goldin, T. Scheuer, and W.A. Catterall. 1997. Dopaminergic modulation of sodium current in hippocampal neurons via cAMP-dependent phosphorylation of specific sites in the sodium channel alpha subunit. *J. Neurosci.* 17:7330–7338.
- Cerda, O., and J.S. Trimmer. 2010. Analysis and functional implications of phosphorylation of neuronal voltage-gated potassium channels. *Neurosci. Lett.* 486:60–67.
- Cohen, P. 2001. The role of protein phosphorylation in human health and disease. The Sir Hans Krebs Medal Lecture. *Eur. J. Biochem.* 268:5001–5010. doi:10.1046/j.0014-2956.2001.02473.x
- Collins, M.O., and S.G. Grant. 2007. Supramolecular signalling complexes in the nervous system. Subcell. Biochem. 43:185–207. doi:10.1007/978-1-4020-5943-8_9
- Costa, M.R., and W.A. Catterall. 1984. Phosphorylation of the alpha subunit of the sodium channel by protein kinase C. Cell. Mol. Neurobiol. 4:291–297. doi:10.1007/BF00733592
- Costa, M.R., J.E. Casnellie, and W.A. Catterall. 1982. Selective phosphorylation of the alpha subunit of the sodium channel by cAMP-dependent protein kinase. *J. Biol. Chem.* 257:7918–7921.
- Dai, S., D.D. Hall, and J.W. Hell. 2009. Supramolecular assemblies and localized regulation of voltage-gated ion channels. *Physiol. Rev.* 89:411–452. doi:10.1152/physrev.00029.2007
- Diella, F., S. Cameron, C. Gemund, R. Linding, A. Via, B. Kuster, T. Sicheritz-Ponten, N. Blom, and T.J. Gibson. 2004. Phospho. ELM: a database of experimentally verified phosphorylation sites in eukaryotic proteins. *BMC Bioinformatics*. 5:79. doi:10.1186/ 1471-2105-5-79
- Diella, F., C.M. Gould, C. Chica, A. Via, and T.J. Gibson. 2008. Phospho.ELM: a database of phosphorylation sites—update 2008. Nucleic Acids Res. 36:D240–D244. doi:10.1093/nar/gkm772
- Fang, H., S. Patanavanich, S. Rajagopal, X. Yi, M.S. Gill, J.J. Sando, and G.L. Kamatchi. 2006. Inhibitory role of Ser-425 of the alpha1 2.2 subunit in the enhancement of Cav 2.2 currents by phorbol-12-myristate, 13-acetate. *J. Biol. Chem.* 281:20011–20017. doi:10.1074/jbc.M601776200
- Gnad, F., S.B. Ren, J. Cox, J.V. Olsen, B. Macek, M. Oroshi, and M. Mann. 2007. PHOSIDA (phosphorylation site database): management, structural and evolutionary investigation, and prediction of phosphosites. *Genome Biol.* 8:R250. doi:10.1186/ gb-2007-8-11-r250
- Gnad, F., L.M. de Godoy, J. Cox, N. Neuhauser, S. Ren, J.V. Olsen, and M. Mann. 2009. High-accuracy identification and bioinformatic analysis of in vivo protein phosphorylation sites in yeast. *Proteomics*. 9:4642–4652. doi:10.1002/pmic.200900144
- Hammond, R.S., L. Lin, M.S. Sidorov, A.M. Wikenheiser, and D.A. Hoffman. 2008. Protein kinase a mediates activity-dependent Kv4.2 channel trafficking. J. Neurosci. 28:7513–7519. doi:10.1523/ JNEUROSCI.1951-08.2008
- Hanlon, M.R., and B.A. Wallace. 2002. Structure and function of voltage-dependent ion channel regulatory beta subunits. *Biochemistry*. 41:2886–2894. doi:10.1021/bi0119565
- Hille, B. 2001. Ionic channels of excitable membranes. Third ed. Sinauer, Sunderland, MA. 814 pp.
- Jarvis, S.E., and G.W. Zamponi. 2001. Distinct molecular determinants govern syntaxin 1A-mediated inactivation and G-protein inhibition of N-type calcium channels. J. Neurosci. 21:2939–2948.
- Johnson, R.P., A.F. El-Yazbi, M.F. Hughes, D.C. Schriemer, E.J. Walsh, M.P. Walsh, and W.C. Cole. 2009. Identification and

- functional characterization of protein kinase A-catalyzed phosphorylation of potassium channel Kv1.2 at serine 449. *J. Biol. Chem.* 284:16562–16574. doi:10.1074/jbc.M109.010918
- Lemeer, S., and A.J. Heck. 2009. The phosphoproteomics data explosion. Curr. Opin. Chem. Biol. 13:414–420. doi:10.1016/j.cbpa.2009.06.022
- Levitan, I.B. 1985. Phosphorylation of ion channels. J. Membr. Biol. 87:177–190. doi:10.1007/BF01871217
- Levitan, I.B. 2006. Signaling protein complexes associated with neuronal ion channels. Nat. Neurosci. 9:305–310. doi:10.1038/nn1647
- Long, S.B., E.B. Campbell, and R. Mackinnon. 2005. Crystal structure of a mammalian voltage-dependent Shaker family K+ channel. Science. 309:897–903. doi:10.1126/science.1116269
- Martin, S.W., A.J. Butcher, N.S. Berrow, M.W. Richards, R.E. Paddon, D.J. Turner, A.C. Dolphin, T.S. Sihra, and E.M. Fitzgerald. 2006. Phosphorylation sites on calcium channel alphal and beta subunits regulate ERK-dependent modulation of neuronal N-type calcium channels. *Cell Calcium*. 39:275–292. doi:10.1016/j.ceca.2005.11.002
- Misonou, H., D.P. Mohapatra, E.W. Park, V. Leung, D. Zhen, K. Misonou, A.E. Anderson, and J.S. Trimmer. 2004. Regulation of ion channel localization and phosphorylation by neuronal activity. *Nat. Neurosci.* 7:711–718. doi:10.1038/nn1260
- Misonou, H., D.P. Mohapatra, M. Menegola, and J.S. Trimmer. 2005. Calcium- and metabolic state-dependent modulation of the voltage-dependent Kv2.1 channel regulates neuronal excitability in response to ischemia. *J. Neurosci.* 25:11184–11193. doi:10.1523/JNEUROSCI.3370-05.2005
- Misonou, H., M. Menegola, D.P. Mohapatra, L.K. Guy, K.S. Park, and J.S. Trimmer. 2006. Bidirectional activity-dependent regulation of neuronal ion channel phosphorylation. *J. Neurosci.* 26:13505–13514. doi:10.1523/JNEUROSCI.3970-06.2006
- Mohapatra, D.P., K.S. Park, and J.S. Trimmer. 2007. Dynamic regulation of the voltage-gated Kv2.1 potassium channel by multisite phosphorylation. *Biochem. Soc. Trans.* 35:1064–1068. doi:10.1042/BST0351064
- Munton, R.P., R. Tweedie-Cullen, M. Livingstone-Zatchej, F. Weinandy, M. Waidelich, D. Longo, P. Gehrig, F. Potthast, D. Rutishauser, B. Gerrits, et al. 2007. Qualitative and quantitative analyses of protein phosphorylation in naive and stimulated mouse synaptosomal preparations. Mol. Cell. Proteomics. 6:283–293.
- Nara, M., P.D.K. Dhulipala, G.J. Ji, U.R. Kamasani, Y.X. Wang, S. Matalon, and M.I. Kotlikoff. 2000. Guanylyl cyclase stimulatory coupling to K-Ca channels. Am. J. Physiol. Cell Physiol. 279:C1938–C1945.
- Park, K.S., D.P. Mohapatra, H. Misonou, and J.S. Trimmer. 2006. Graded regulation of the Kv2.1 potassium channel by variable phosphorylation. *Science*. 313:976–979. doi:10.1126/science.1124254
- Prasad, T.S.K., R. Goel, K. Kandasamy, S. Keerthikumar, S. Kumar, S. Mathivanan, D. Telikicherla, R. Raju, B. Shafreen, A. Venugopal, et al. 2009. Human Protein Reference Database-2009 update. Nucleic Acids Res. 37:D767–D772. doi:10.1093/nar/gkn892
- Rajagopal, S., H. Fang, C.I. Oronce, S. Jhaveri, S. Taneja, E.M. Dehlin, S.L. Snyder, J.J. Sando, and G.L. Kamatchi. 2009. Site-specific regulation of CA(V)2.2 channels by protein kinase C isozymes betaII and epsilon. *Neuroscience*. 159:618–628. doi:10.1016/j.neuroscience.2008.12.047
- Redman, P.T., K. He, K.A. Hartnett, B.S. Jefferson, L. Hu, P.A. Rosenberg, E.S. Levitan, and E. Aizenman. 2007. Apoptotic surge of potassium currents is mediated by p38 phosphorylation of Kv2.1. Proc. Natl. Acad. Sci. USA. 104:3568–3573. doi:10.1073/pnas.0610159104
- Rinehart, J., Y.D. Maksimova, J.E. Tanis, K.L. Stone, C.A. Hodson, J. Zhang, M. Risinger, W. Pan, D. Wu, C.M. Colangelo, et al. 2009. Sites of regulated phosphorylation that control K-Cl cotransporter activity. *Cell.* 138:525–536. doi:10.1016/j.cell.2009.05.031

- Saneyoshi, T., D.A. Fortin, and T.R. Soderling. 2010. Regulation of spine and synapse formation by activity-dependent intracellular signaling pathways. *Curr. Opin. Neurobiol.* 20:108–115. doi:10.1016/j.conb.2009.09.013
- Schrader, L.A., A.E. Anderson, A. Mayne, P.J. Pfaffinger, and J.D. Sweatt. 2002. PKA modulation of Kv4.2-encoded A-type potassium channels requires formation of a supramolecular complex. *J. Neurosci.* 22:10123–10133.
- Schroeder, B.C., C. Kubisch, V. Stein, and T.J. Jentsch. 1998. Moderate loss of function of cyclic-AMP-modulated KCNQ2/KCNQ3 K+ channels causes epilepsy. *Nature*. 396:687–690. doi:10 1038/95367
- Schulz, D.J., S. Temporal, D.M. Barry, and M.L. Garcia. 2008. Mechanisms of voltage-gated ion channel regulation: from gene expression to localization. *Cell. Mol. Life Sci.* 65:2215–2231. doi:10.1007/s00018-008-8060-z
- Seikel, E., and J.S. Trimmer. 2009. Convergent modulation of Kv4.2 channel alpha subunits by structurally distinct DPPX and KChIP auxiliary subunits. *Biochemistry*. 48:5721–5730. doi:10 .1021/bi802316m
- Shah, M.M., R.S. Hammond, and D.A. Hoffman. 2010. Dendritic ion channel trafficking and plasticity. *Trends Neurosci.* 33:307–316. doi:10.1016/j.tins.2010.03.002
- Smith, R.D., and A.L. Goldin. 1997. Phosphorylation at a single site in the rat brain sodium channel is necessary and sufficient for current reduction by protein kinase A. J. Neurosci. 17:6086–6093.
- Surti, T.S., L. Huang, Y.N. Jan, L.Y. Jan, and E.C. Cooper. 2005. Identification by mass spectrometry and functional characterization of two phosphorylation sites of KCNQ2/KCNQ3 channels. *Proc. Natl. Acad. Sci. USA*. 102:17828–17833. doi:10.1073/pnas.0509122102
- Trimmer, J.S. 1991. Immunological identification and characterization of a delayed rectifier K+ channel polypeptide in rat brain. *Proc. Natl. Acad. Sci. USA.* 88:10764–10768. doi:10.1073/pnas.88.23.10764
- Trinidad, J.C., A. Thalhammer, C.G. Specht, A.J. Lynn, P.R. Baker, R. Schoepfer, and A.L. Burlingame. 2008. Quantitative analysis of synaptic phosphorylation and protein expression. *Mol. Cell. Proteomics*. 7:684–696.
- Turrigiano, G.G. 2008. The self-tuning neuron: synaptic scaling of excitatory synapses. *Cell.* 135:422–435. doi:10.1016/j.cell.2008 .10.008
- Tweedie-Cullen, R.Y., J.M. Reck, and I.M. Mansuy. 2009. Comprehensive mapping of post-translational modifications on synaptic, nuclear, and histone proteins in the adult mouse brain. *J. Proteome Res.* 8:4966–4982. doi:10.1021/pr9003739
- Ubersax, J.A., and J.E. Ferrell Jr. 2007. Mechanisms of specificity in protein phosphorylation. *Nat. Rev. Mol. Cell Biol.* 8:530–541. doi:10.1038/nrm2203
- Vacher, H., D.P. Mohapatra, and J.S. Trimmer. 2008. Localization and targeting of voltage-dependent ion channels in mammalian central neurons. *Physiol. Rev.* 88:1407–1447. doi:10.1152/physrev .00002.2008
- Wang, H., W.J. Qian, M.H. Chin, V.A. Petyuk, R.C. Barry, T. Liu, M.A. Gritsenko, H.M. Mottaz, R.J. Moore, D.G. Camp Ii, et al. 2006. Characterization of the mouse brain proteome using global proteomic analysis complemented with cysteinyl-peptide enrichment. J. Proteome Res. 5:361–369. doi:10.1021/pr0503681
- Wisniewski, J.R., A. Zougman, N. Nagaraj, and M. Mann. 2009. Universal sample preparation method for proteome analysis. *Nat. Methods*. 6:359–362. doi:10.1038/nmeth.1322
- Wisniewski, J.R., N. Nagaraj, A. Zougman, F. Gnad, and M. Mann. 2010. Brain phosphoproteome obtained by a FASP-based method reveals plasma membrane protein topology. *J. Proteome Res.* 9:3280–3289. doi:10.1021/pr1002214

- Yan, J., J.V. Olsen, K.S. Park, W. Li, W. Bildl, U. Schulte, R.W. Aldrich, B. Fakler, and J.S. Trimmer. 2008. Profiling the phospho-status of the BKCa channel alpha subunit in rat brain reveals unexpected patterns and complexity. *Mol. Cell. Proteomics*. 7:2188–2198. doi:10 .1074/mcp.M800063-MCP200
- Yang, J.W., H. Vacher, K.S. Park, E. Clark, and J.S. Trimmer. 2007. Trafficking-dependent phosphorylation of Kv1.2 regulates voltage-gated potassium channel cell surface expression. *Proc. Natl. Acad. Sci. USA*. 104:20055–20060. doi:10.1073/pnas.0708574104
- Yokoyama, C.T., S.J. Myers, J. Fu, S.M. Mockus, T. Scheuer, and W.A. Catterall. 2005. Mechanism of SNARE protein binding
- and regulation of Cav2 channels by phosphorylation of the synaptic protein interaction site. *Mol. Cell. Neurosci.* 28:1–17. doi:10.1016/j.mcn.2004.08.019
- Yu, F.H., V. Yarov-Yarovoy, G.A. Gutman, and W.A. Catterall. 2005. Overview of molecular relationships in the voltage-gated ion channel superfamily. *Pharmacol. Rev.* 57:387–395. doi:10 .1124/pr.57.4.13
- Zhou, X.B., I. Wulfsen, E. Utku, U. Sausbier, M. Sausbier, T. Wieland, P. Ruth, and M. Korth. 2010. Dual role of protein kinase C on BK channel regulation. *Proc. Natl. Acad. Sci. USA*. 107:8005–8010. doi:10.1073/pnas.0912029107